SvedbergOpen
DISSEMINATION OF KNOWLEDGE
International Journal of Artificial Intelligence and Machine Learning
Publisher's Home Page: https://www.svedbergopen.com/
Research Paper
Open Access

A Comparative Study Of Statistical And Machine Learning Approaches For Landslide Susceptibility Zonation In A Hilly Region

Swati Punyal[1], Dr. Parveen Kumar[2]

[1*]Swati Punyal, PhD Scholar, Department of Architecture, DCRUST, Murthal, spunyal@gmail.com
[2]Dr. Parveen Kumar, Professor, Department of Architecture, DCRUST, Murthal, parveenkumar.arch@dcrustm.org
[*]Corresponding Author: Swati Punyal, spunyal@gmail.com

Abstract
The North-Western Himalayas are prone to Landslides due to extreme climatic conditions and human interventions. These areas are particularly susceptible to disasters due to steep slopes, complex geological features, heavy rainfall, and urban expansion. It's crucial to identify the areas that are most at risk to manage disasters effectively and plan for the community's safety. This study uses a GIS approach to analyse seventeen major factors contributing to landslides, including landscape, environmental conditions, and human activities. By employing methods such as Information Value and Weight of Evidence, the study examined the relationships between these factors and past landslides and refined the predictions using the Frequency Ratio. The AUC-ROC curve analysis of the validation with historical data shows that the resulting susceptibility map is a valuable tool for guiding development and mitigating disaster risks in these vulnerable areas. Future research will quantify the effects of anthropogenic influences on slope instability to better understand human-induced contributions to landslide risk in rapidly urbanizing mountain environments.

Keywords: Landslide Susceptibility, GIS, Solan District, Information Value, Weight of Index, Frequency Ratio Method, AUC-ROC Curve.

1. Introduction

In hilly areas around the world, landslides are among the most common and destructive natural hazards, posing serious risks to infrastructure, agriculture, ecosystems, and human life (Petley, 2018). Landslides are frequent and frequently disastrous in the geologically delicate Western Himalayas because of the interaction of man-made and natural causes (Anbalagan, 2015). The Solan District of Himachal Pradesh, part of this sensitive mountain belt, has emerged as a particularly vulnerable region. Due to the district's steep slopes, delicate lithology, strong seismicity, and heavy monsoonal rainfall, the number of landslides has significantly increased during the last few decades (Mahesh Sharma, 2024) ((NIDM), 2020).

Solan's strategic location along the Shivalik and Lesser Himalayan ranges makes it geologically complex (GSI, 2023). Sandstone, shale, and phyllite are among the sedimentary and metamorphic rocks that make up the region; these rocks are highly vulnerable to weathering and erosion (Valdiya, 1980). These formations, in conjunction with tectonic activity and heavy precipitation events, create conditions that predispose the region to landslides. Moreover, the construction of roads, buildings, and industrial zones along vulnerable slopes without adequate geological assessment has further increased the likelihood of slope failures. According to the Geological Survey of India (GSI) and the Himachal Pradesh State Disaster Management Authority (HPSDMA), landslides in Solan have frequently caused fatalities, damaged property, interrupted transit, and jeopardised livelihoods. For example, roadblocks due to landslides along the National Highway 5 and the Kalka-Shimla railway line have become increasingly frequent during the monsoon season (HPSDMA, 2023 & 2024).

Accurately delineating landslide susceptible zones is crucial in this complex landscape. This work addresses the need for accurate spatial analysis by developing a thorough landslide susceptibility map for the Solan District. The

Geographic Information System (GIS) approach is essential for evaluating the natural hazards and spatial analysis as it allows for the integration, analysis as well as visualization of various spatial datasets. The study uses a multi-criteria evaluation approach while incorporating 17 causative factors that influence landslide occurrence (Tesfaldet Sisay, 2024). These 17 factors are categorised into 5 main categories: Geological (lithology, fault proximity), hydrological (drainage density, distance from rivers), topographical (elevation, slope, aspect, curvature), environmental (rainfall, vegetation cover) and anthropogenic (road density, built-up area, land use/land cover changes) are the five main categories of these factors. Each of these factors contributes uniquely to slope instability as their spatial relationships are analyzed through statistical modeling (Adil Ahmad Magray K. S., 2023).

This study uses a hybrid modelling framework to understand the factors influencing landslide susceptibility. It combines the Information Value (IV), Weight of Evidence (Woe), and Frequency Ratio (FR) methods (Kumari Sweta, 2022). The Information Value method is used first which depicts how each environmental factor aligned with known landslide sites. Factors showing a stronger link were given higher weights. The Weight of Evidence technique was then applied to refine the results. This probabilistic method made it possible to check whether each factor was likely to raise or lower the chances of slope failure (Bharat Prasad Bhandari, 2024). Thorough field observations and high-resolution imagery available on Google Earth Engine were used to ensure that the mapped landslides reflected actual conditions. The Frequency Ratio method compared how often landslides occurred within each class with that class's area. This method made it easier to identify the specific conditions that caused more of the slope failure (Yuqian Yang, 2024). Combining all these methods produced a more dependable picture of landslide behaviour which was consistent with approaches used elsewhere in the Himalayan regions (Zare, 2014). The final susceptibility map for Solan District divides the landscape into five classes ranging from very low to very high. The AUC-ROC curve analysis showed a strong match between predicted vulnerability and observed events. Hence, it underlined the model's usefulness for hazard reduction and land-use planning.

The paper also emphasizes the role of human interventions in destabilizing slopes. Hilly regions like the Solan district where practices such as slope cutting and vegetation clearing are worsening local geomorphic conditions. There is a need for regular slope-stability monitoring as a part of urban planning and development decisions (Vipin Chauhan, 2024). The study focuses on how built-up expansion relates to landslide patterns across the area. The results show how unregulated human intervention often disturbs the balance of fragile hill slopes, making them more prone to failure (Saibal Ghosh, 2012) (Fig.1). These findings also resonate with national-level recommendations advocating for the integration of geohazard mapping into developmental planning across the Indian Himalayan Region (Sati, 2019). The study also aligns with the context of climate change events escalating landslide risks in the Himalayan region (Thakur, 2025). High-resolution spatial datasets and model outputs are used in this study to establish a robust baseline for long-term monitoring and adaptive landscape management strategies in such hilly terrains. Hence, the research bridges scientific analysis and policy-relevant application for delivering a reliable landslide susceptibility model. This model will guide disaster risk reduction, infrastructure planning and sustainable development in Solan and similar vulnerable mountain environments.

Figure 1 NH-05 Road Affected Near Koti area (Between Parwanoo to Sanwari) in 2023.
(Source: HPSDMA and analyzed by the author.)

Figure 2 Location Map of the Study Area. (Source: Author)

Figure 3 Landslide Inventory of Solan District. (Source: GSI-Bhukosh, HPSDMA and Field Documentation by Author)

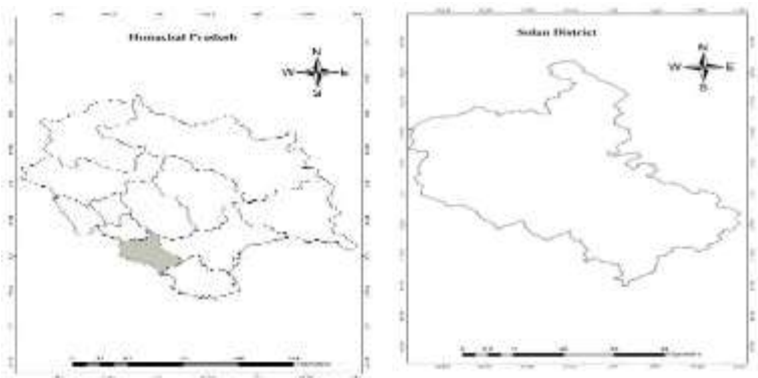

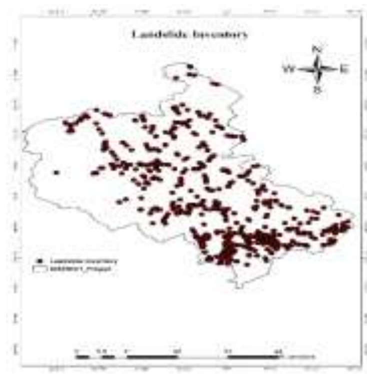

2. Study Area

Solan district is on the south-western side of Himachal Pradesh, which stretches roughly from 30.9° to 31.3° N and 76.7° to 77.2° E (Fig 2). It covers an area of 1,936 square kilometers. The terrain rises sharply from about 300 meters in the lower valleys to a little above 2,100 meters on the surrounding hilltops. The climate is best described as subtropical highland. Rainfall is relatively high, more than 1,200 millimeters a year, and most of it arrives with the summer monsoon between June and September. The terrain is highly dissected with steep slopes and fragile geological formations. These dissected slopes are predominantly of the Krol, Shali and Simla groups. Rapid urban development along the Kalka-Shimla corridor and in towns like Solan, Parwanoo and Kasauli has increased slope instability (HPSDMA, 2023 & 2024) (Fig. 4).

Figure 4 Field Survey -Dharampur- Subathu- Kunihar Road and Sabathu Military Area affected due to heavy rainfall.
(Source: HPSDMA, New Articles and Author)

Landslides have become a familiar problem in Solan district during the spells of heavy monsoon rain. In July 2025, several slopes were affected along National Highway-5 between Dharampur and Solan after extreme rainfall. Traffic along the main highway was affected with few roadside buildings were damaged. Issues of water collection were also reported in some low stretches of the road. One large slide buried the highway under debris, which affected the traffic movement for eighteen hours near Kandaghat town. In June 2025, before the July incidents, a landslide near Jabli disrupted the Kalka–Shimla railway line and damaged a few hillside houses. Such failures have occurred repeatedly in recent years. Much of it seems linked to hill cutting for construction, poor drainage planning and the weak weathered rock that makes up much of the local terrain. According to recent alerts issued by the Himachal Pradesh State Disaster Management Authority (HPSDMA), Solan remains one of the highest-risk districts in the Western Himalayas. What happened shows the need to understand where the ground is weakest and to plan development accordingly. Mapping the risky areas first could help prevent more losses across Solan in the years ahead.

`3. Data Collection

3.1 Landslide Inventory of Solan District

The landslide inventory for Solan district was mapped using verified reports from the Himachal Pradesh State Disaster Management Authority (HPSDMA) and the Geological Survey of India (GSI). The database covers landslides that occurred between 2012 and 2024 monsoon. Most of these landslides occurred along NH-5 and the Kalka–Shimla rail line, with several others reported near Kandaghat, Dharampur and Kasauli sub-district. The main causes identified were the steep local slopes, weak rock formations and increasing human pressure due to road cutting and the removal of forest cover. A total of 795 landslide points were digitized and georeferenced in a GIS environment. Out of which 630 points were used for model training and 165 were retained for validation using success rate and ROC–AUC curve analysis. This inventory provides a strong empirical basis for applying the Information Value (IV), Weight of Evidence (WoE) and Frequency Ratio (FR) methods in landslide susceptibility modelling across the district (Abdullah H. Alsabhana, 2022).

3.2 Causative Factors Governing Landslide Occurrence

A single cause does not trigger landslides in mountainous terrain such as the Solan district. Landslides are the result of complex interactions among a multitude of natural and anthropogenic factors (Adil Ahmad Magray K. S., 2023). In this study, seventeen landslide conditioning factors were carefully selected and categorized into four broad groups: topographical, environmental and anthropogenic, geological and soil characteristics, and hydrological (Fig. 5) (Lalit Pathak, 2025) (Pham Viet Hoa, 2023). Each factor influences slope stability in its own way. A brief discussion of these aspects is given in the following section:

3.2.1 Topographical Factors

a) **Slope:** Steeper slopes are more susceptible to landslides as the pressure on the hill material increases, which makes the ground more likely to give way. In the Solan District, slopes steeper than about 30 degrees tend to fail more easily after heavy rains or when the surface has been disturbed by construction or cutting.

b) **Aspect:** Aspect controls the amount of solar radiation and moisture content in hilly region. South and south-west-facing slopes typically receive more sunlight. This affects the evapotranspiration rates and soil moisture content. Therefore, it often alters the cohesion and weight of slope materials.

c) **Elevation:** The change in altitude showed a noticeable change in the type of rocks and landforms present. The higher altitude regions of the district experience greater erosion and occasional rockfalls. Whereas the lower areas tend to accumulate loose material and retain more moisture after rainfall.

d) **Curvature:** Curvature study governs whether the ground surface is inward or outward. Rainwater runoff is faster on the convex surface, which cuts into the surface and causes slope failure. A concave surface holds onto water and loose debris, which can raise the soil's moisture content and pressure, weakening the slope.

3.2.2 Anthropogenic and Environmental Factors

e) **Land Use/Land Cover (LULC):** Human interventions such as deforestation, road construction and urban expansion modify natural slopes. The landslide inventory highlighted that built-up and agricultural areas are more prone to landslides due to vegetation loss and surface compaction.

f) **Normalized Difference Vegetation Index (NDVI), Built-up Index (NDBI) and Water Index (NDWI):**
NDVI: Vegetation cover is reflected in the NDVI layer. Low NDVI values indicate sparse vegetation that affects slope stability.
NBDI: Urbanisation levels are shown by the NBDI. Increased anthropogenic involvement and high NDBI levels often lead to destabilisation.
NDWI: Road infrastructure construction frequently causes instability by affecting the slope's toe. Excavation, poor drainage and road-related vibrations all significantly raise the danger of landslides.

g) **Distance from Road:** Construction of road infrastructure often disturbs the toe of the slope which causes slope instability. The risk of landslides is greatly increased by road-related vibrations, excavation, and poor drainage.

3.2.3 Geological and Soil Characteristics

h) Lithology: The composition and structure of various rock types have a direct impact on slope resistance. Weak and worn rocks that are particularly vulnerable to disintegration under stress include schist and shale rocks.

i) Geomorphology: Surface processes and landform types are included in geomorphology study. Escarpments, ridgelines and dissected hills are examples of zones that are typically more unstable than depositional or gently sloping areas.

j) Distance from Lineament: Distance from lineament study highlights the water infiltration which indicates the geological faults or fractures. Close proximity of lineaments to the surface depicts slope weakness and mechanical weathering.

k) Soil Texture: The cohesion and permeability differs in different soil types. Landslides are more susceptible in loose, sandy soils and silty materials because they are less cohesive and more vulnerable to liquefaction or erosion.

3.2.4 Hydrological Factors

l) Rainfall: In Solan, one of the most important causes of landslides during the monsoon season. Slope failure results from heavy rainfall due to saturation, reduced matric suction and elevated pore-water pressure.

m) Topographic Wetness Index (TWI): The TWI study represents the spatial distribution of soil moisture. Areas with high TWI values are more prone to landslides as Water builds up in such areas. This increases the saturation and reduces the soil strength thereby leading to increased risk of landslides.

n) Stream Power Index (SPI): The SPI study in hilly terrains depicts the erosive force of overland flow. Since soil detachment and gully formation are frequent precursors to slope failure, higher SPI values are typically observed near stream channels or in areas with concentrated runoff.

o) Distance from Stream: Hilly areas near streams are subject to undercutting and toe erosion. This weakens the slope support from below, triggering rotational and translational slides

Figure 5 Thematic Layers, Slope, Aspect, Elevation, Curvature, Road Distance, Lithology, Geomorphology, Lineament Distance, Soil Texture, Rainfall, TWI, SPI, LULC 2024, NDVI, NDBI, NDWI, Drainage Distance, Site photos

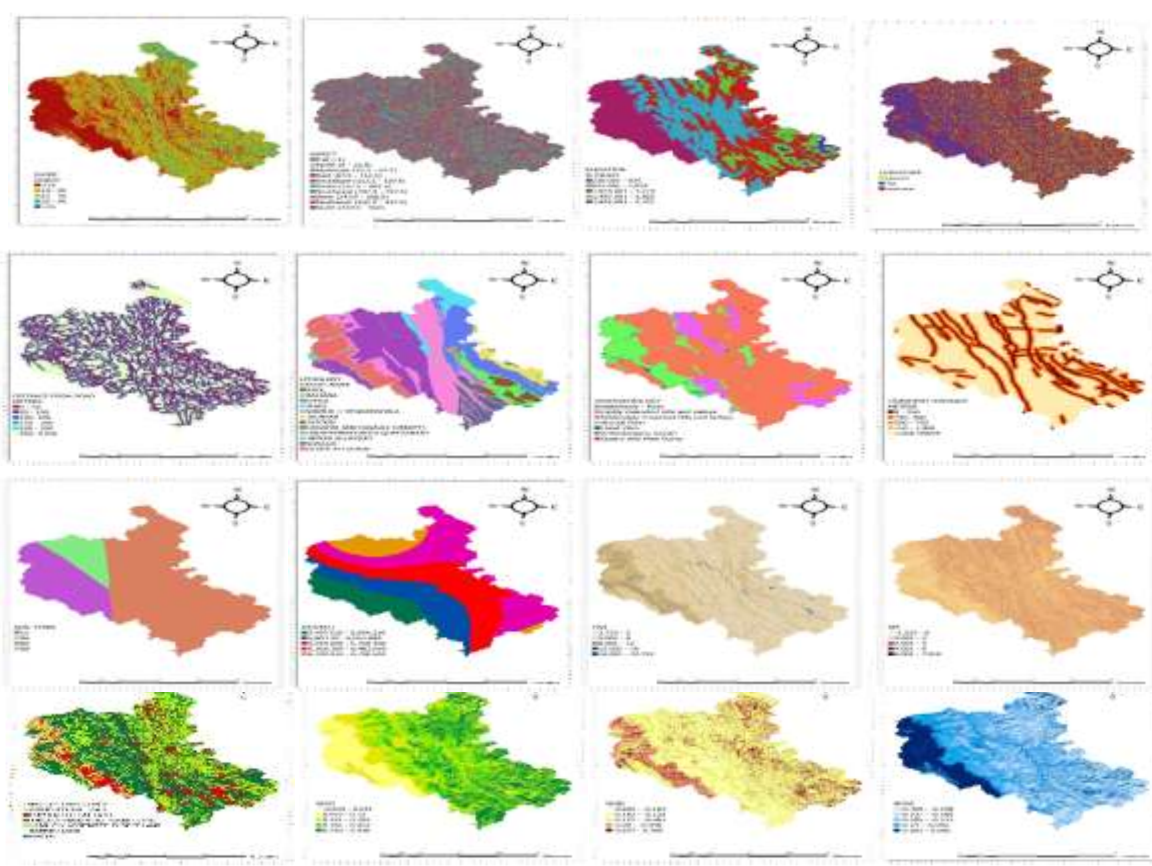

3. Methodology

Frequency Ratio (FR), Information Value (IV), and Weight of Evidence (WoE) are three well-known bivariate statistical models used in this study's hybrid multi-model framework for landslip susceptibility zonation (LSZ). Thematic layers extracted from spatial datasets were used to apply these techniques, and they were verified against a Solan district landslide inventory (Fig 6).

Figure 6 Methodology Chart for Landslide Susceptibility Zonation. (Source: Author)

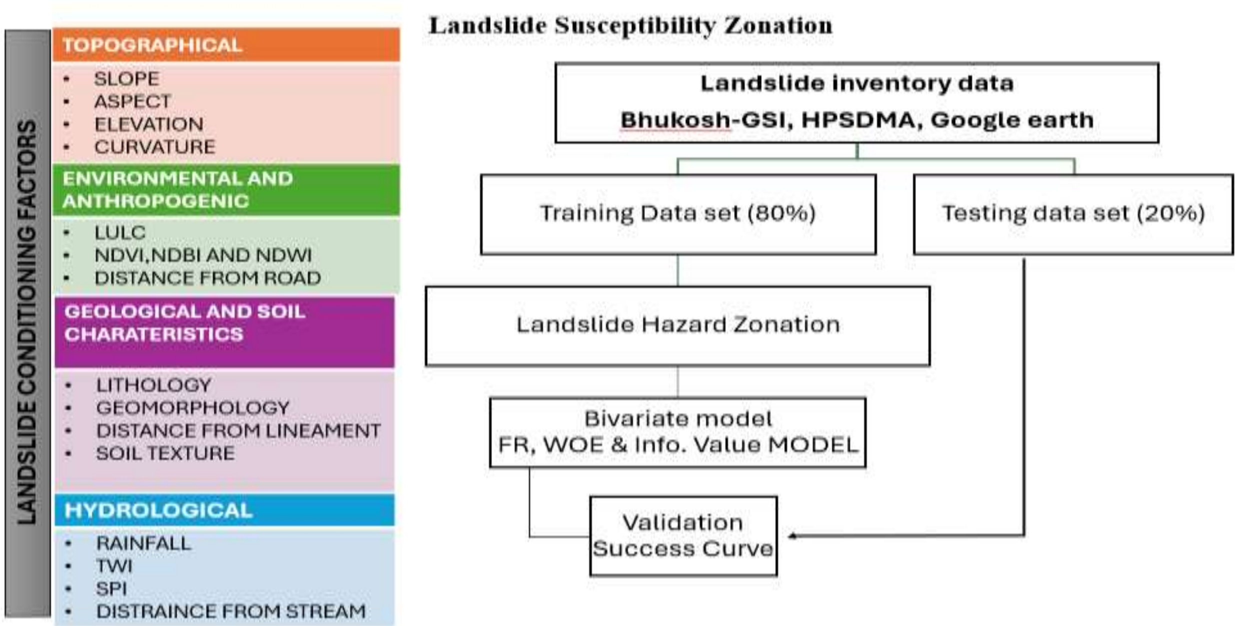

4.1 Frequency Ratio (FR) Method

FR is a bivariate geo-statistical method to compute the probabilistic correlation between independent and dependent variables

The following equation has been used to compute the recurrence fraction (FR) for each class of origin.

$$Fr = \frac{\frac{Count(C)}{NCount}}{\frac{Landslide\ (L)}{PLandslide}}$$

Count (C)= the class's total pixels that are covered by landslides.

NCount= the sum of all pixels in all classes

Landslide (L) = Count of all pixels containing landslide

Plandslide = Count of all pixels

By using the equation below to sum the estimated frequency ratios, a map of the landslide susceptibility index can be generated. (LSI):

$$LSI = Fr1 + Fr2 + Fr3 + Fr4 + \cdots + Frn$$

Here, n denotes the aggregates of causal features chosen, and Fr symbolises the frequency ratio.

Slope (Degree)	Count (C)	Landslide (L)	FR
<15	756385	42	0.19
15-25	690674	196	0.97
25-35	539808	274	1.73
35-45	146356	107	2.49
>45	15166	11	2.47
Aspect	**Count (C)**	**Landslide (L)**	**FR**
Flat (-1)	0	0	0.00
North (0 - 22.5)	123021	27	0.75
Northeast (22.5 - 67.5)	269621	76	0.96
East (67.5 - 112.5)	250070	80	1.09
Southeast (112.5 - 157.5)	218151	55	0.86
South (157.5 - 202.5)	264168	80	1.03
Southwest (202.5 - 247.5)	333155	130	1.33
West (247.5 - 292.5)	321332	103	1.09
Northwest (292.5 - 337.5)	260133	47	0.62
Northwest (292.5 - 337.5)	108738	32	1.00
Curvature	**Count (C)**	**Landslide (L)**	**FR**
Convex	356185	132	1.26
Flat	764299	176	0.79
Concave	1027905	322	1.07
Geomorphology	**Count (C)**	**Landslide (L)**	**FR**
Waterbody – River	31544	3	0.32
Highly Dissected Hills and Valleys	1532348	537	1.20
Moderately Dissected Hills and Valleys	223359	60	0.92
Alluvial Plain	347204	30	0.29
Flood Plain	10914	0	0.00
Anthropogenic terrain	564	0	0.00
Quarry and Mine Dump	2456	0	0.00
TWI	**Count (C)**	**Landslide (L)**	**FR**
2.70-5.0	762752	356	1.59
5.0-8.0	1080934	244	0.77
8.0-12.0	241558	26	0.37
12.0-16.0	52504	2	0.13
16-23.72	10641	2	0.64
SPI	**Count (C)**	**Landslide (L)**	**FR**
-1.522879	76066	0	0.00
0-2.0	1615313	498	1.05
2.0-4.0	433668	129	1.01
4.0-6.0	22929	2	0.30
6.0-7.01	413	1	8.26
LINEAMENT DISTANCE	**Count (C)**	**Landslide (L)**	**FR**
0-250	309340	106	1.17
250-500	273762	89	1.11
500-750	246615	50	0.69
750-100	219621	42	0.65
1000 ABOVE	1099051	343	1.06
ROAD	**Count (C)**	**Landslide (L)**	**FR**
0-50	398733	522	4.46
50-100	321487	62	0.66
100-150	265797	12	0.15
150-200	182428	12	0.22

200-250	192690	9	0.16
250 above	787254	13	0.06
SOIL TYPE	**Count (C)**	**Landslide (L)**	**FR**
Orthic Luvisols (Lo)	466582	16	0.12
Eutric Regosols (Re)	218832	62	0.97
Eutric Cambisols (Be)	1462454	552	1.29
Dystric Cambisols (Bd)	521	0	0.00
NDVI	**Count (C)**	**Landslide (L)**	**FR**
-0.019 – 0.041	5978	0	0.00
0.042 – 0.120	374140	50	0.46
0.121 – 0.183	605775	237	1.33
0.184 – 0.242	724739	225	1.06
0.243 – 0.438	437757	118	0.92
NDBI	**Count (C)**	**Landslide (L)**	**FR**
-0.292 to -0.163	421756	152	1.23
-0.162 to -0.122	628600	213	1.16
-0.121 to -0.081	535282	140	0.89
-0.080 to -0.038	400747	97	0.83
-0.037 to 0.286	162004	28	0.59
NDWI	**Count (C)**	**Landslide (L)**	**FR**
-0.409 to -0.238	214690	61	0.97
-0.237 to -0.186	428933	136	1.08
-0.185 to -0.141	572580	163	0.97
-0.140 to -0.092	521201	202	1.32
-0.091 to -0.066	410985	68	0.56
DRAINAGE DISTANCE	**Count (C)**	**Landslide (L)**	**FR**
0-250	724460	208	0.98
250-500	572537	151	0.90
500-750	434254	130	1.02
750-1000	279334	102	1.25
1000 ABOVE	137804	39	0.97
Rainfall Range (mm)	**Count (C)**	**Landslide (L)**	**FR**
5,487.515 – 5,804.319	285362	17	0.20
5,804.32 – 6,054.698	436107	216	1.69
6,054.699 – 6,269.308	583849	210	1.23
6,269.309 – 6,483.918	657361	146	0.76
6,483.919 – 6,790.504	185710	41	0.75
LITHOLOGY	**Count (C)**	**Landslide (L)**	**FR**
KROL	61321	18	1.00
BALIANA	108360	41	1.29
SIMLA	301602	79	0.89
SHALI	123922	9	0.25
SIRMUR = DHARAMSHALA	498951	235	1.61
JAUNSAR	74753	5	0.23
JUTOGH	4495	2	1.52
DAGSHAI AND KASAULI (UNDIFF)	121834	101	2.83
UNDIFFERENTIATED QUATERNARY	14030	1	0.24
NEWER ALLUVIUM	50792	6	0.40
SIWALIK	540760	132	0.83
OLDER ALLUVIUM	247569	1	0.01

ELEVATION	**Count (C)**	**Landslide (L)**	**FR**
226-625	504604	31	0.2
625-1024	636384	204	1.1
1024-1423	703752	267	1.3
1423-1822	270978	125	1.6
1822-2221	32671	3	0.31
Land Cover Class	**Count (C)**	**Landslide (L)**	**FR**
Water Body	27939	4	0.49
forest	894437	242	0.92
agriculture	142314	0	0.00
Built-up / Settlement	366150	210	1.96
Barren	810	0	0.00
moderate to sparse vegetation	716739	174	0.83

5.2 Information Value (IV) Method

In the Information Value (IV) approach, the relationship between landslide events and the different classes of each conditioning factor is examined through a comparison of their respective densities. The IV corresponding to a particular class i is then derived using the following expression:

$IV_i = \ln[(Si / S) / (Ni / N)]$

Where:

- Si = number of landslide pixels in class i
- Ni = number of pixels in class i
- S = total landslide pixels in the study area
- N = total number of pixels in the study area

Positive IV values indicate higher landslide susceptibility, while negative values imply lower susceptibility. The IV scores were assigned to corresponding raster layers using ArcGIS Pro's Lookup tool, and summed to generate the final IV-based LSI

SLOPE(Degree)	Count (C)	Landslide (L)	IV
<15	756385	42	-1.664127169
15-25	690674	196	-0.032799555
25-35	539808	274	0.548668304
35-45	146356	107	0.913540543
>45	15166	11	0.905592911
	2148389	630	
ASPECT	**Count (C)**	**Landslide (L)**	**IV**
Flat (-1)	0	0	0
North (0 - 22.5)	123021	27	-0.289764488
Northeast (22.5 - 67.5)	269621	76	-0.03953021
East (67.5 - 112.5)	250070	80	0.087039475
Southeast (112.5 - 157.5)	218151	55	-0.15110058
South (157.5 - 202.5)	264168	80	0.032195089
Southwest (202.5 - 247.5)	333155	130	0.285680322
West (247.5 - 292.5)	321332	103	0.08900785
Northwest (292.5 - 337.5)	260133	47	-0.484291718
Northwest (292.5 - 337.5)	108738	32	0.003548302
	2148389	630	
CURVATURE	**Count (C)**	**Landslide (L)**	**IV**
Convex	356185	132	0.234105382
Flat	764299	176	-0.24172136
Concave	1027905	322	0.066027235
	2148389	630	
GEOMORPHOLOGY	**Count (C)**	**Landslide (L)**	**IV**
Waterbody - River	31544	3	-1.126017389
Highly Dissected Hills and Valleys	1532348	537	0.178195335
Moderately Dissected Hills and Valleys	223359	60	-0.087682062
Alluvial Plain	347204	30	-1.221961403
Flood Plain	10914	0	0
Anthropogenic terrain	564	0	0
Quarry and Mine Dump	2456	0	0
	2148389	630	
TWI	**Count (C)**	**Landslide (L)**	**IV**
2.70-5.0	762752	356	0.464751504
5.0-8.0	1080934	244	-0.261658817
8.0-12.0	241558	26	-1.002259353
12.0-16.0	52504	2	-2.040988458
16-23.72	10641	2	-0.444813565
	2148389	630	
SPI	**Count (C)**	**Landslide (L)**	**IV**
-1.522879	76066	0	0
0-2.0	1615313	498	0.050069771
2.0-4.0	433668	129	0.014286859
4.0-6.0	22929	2	-1.212501586
6.0-7.01	413	1	2.111061405
	2148389	630	

Lineament distance	**Count (C)**	**Landslide (L)**	**IV**
0-250	309340	106	0
250-500	273762	89	0.103130972
500-750	246615	50	-0.369051692
750-100	219621	42	-0.427479997
1000 ABOVE	1099051	343	0.062281807
	2148389	630	
ROAD	**Count (C)**	**Landslide (L)**	**IV**
0-50	398733	522	0
50-100	321487	62	-0.419069004
100-150	265797	12	-1.871072491
150-200	182428	12	-1.494695206
200-250	192690	9	-1.837104384
250 above	787254	13	-2.876847865
	2148389	630	
SOIL TYPE	**Count (C)**	**Landslide (L)**	**IV**
Orthic Luvisols (Lo)	466582	16	-2.146091341
Eutric Regosols (Re)	218832	62	-0.034416209
Eutric Cambisols (Be)	1462454	552	0.252430639
Dystric Cambisols (Bd)	521	0	0
	2148389	630	
NDVI	**Count (C)**	**Landslide (L)**	**IV**
-0.019 – 0.041	5978	0	0
0.042 – 0.120	374140	50	-0.785853335
0.121 – 0.183	605775	237	0.28830523
0.184 – 0.242	724739	225	0.057042531
0.243 – 0.438	437757	118	-0.084225619
	2148389	630	
NDBI	**Count (C)**	**Landslide (L)**	**IV**
-0.292 to -0.163	421756	152	0
-0.162 to -0.122	628600	213	0.14455076
-0.121 to -0.081	535282	140	-0.11439757
-0.080 to -0.038	400747	97	-0.191865608
-0.037 to 0.286	162004	28	-0.528662798
	2148389	630	
NDWI	**Count (C)**	**Landslide (L)**	**IV**
-0.409 to -0.238	214690	61	0
-0.237 to -0.186	428933	136	0.078107875
-0.185 to -0.141	572580	163	-0.029648544
-0.140 to -0.092	521201	202	0.278885652
-0.091 to -0.066	410985	68	-0.572295294
	2148389	630	
DRAINAGE DISTANCE	**Count (C)**	**Landslide (L)**	**IV**
0-250	724460	208	0
250-500	572537	151	-0.106043807
500-750	434254	130	0.020658553
750-1000	279334	102	0.219318333
1000 ABOVE	137804	39	-0.035517021
	2148389	630	
Rainfall Range (mm)	**Count (C)**	**Landslide (L)**	**IV**
5,487.515 – 5,804.319	285362	17	0

5,804.32 – 6,054.698	436107	216	0.5241445
6,054.699 – 6,269.308	583849	210	0.204218862
6,269.309 – 6,483.918	657361	146	-0.277872995
6,483.919 – 6,790.504	185710	41	-0.283860532
	2148389	630	
LITHOLOGY	**Count (C)**	**Landslide (L)**	**IV**
KROL	61321	18	0
BALIANA	108360	41	0.254866768
SIMLA	301602	79	-0.112906696
SHALI	123922	9	-1.39567404
SIRMUR = DHARAMSHALA	498951	235	0.473831338
JAUNSAR	74753	5	-1.477997714
JUTOGH	4495	2	0.416935231
DAGSHAI AND KASAULI (UNDIFF)	121834	101	1.039214773
UNDIFFERENTIATED QUATERNARY	14030	1	-1.414444176
NEWER ALLUVIUM	50792	6	-0.909225674
SIWALIK	540760	132	-0.183419916
OLDER ALLUVIUM	247569	1	-4.284935612
	2148389	630	
ELEVATION	**Count (C)**	**Landslide (L)**	**IV**
226-625	504604	31	0
625-1024	636384	204	0.089071558
1024-1423	703752	267	0.257576356
1423-1822	270978	125	0.453029819
1822-2221	32671	3	-1.161121827
	2148389	630	
Land Cover Class	**Count (C)**	**Landslide (L)**	**IV**
Water Body	27939	4	0
forest	894437	242	-0.080503025
agriculture	142314	0	0
Built-up / Settlement	366150	210	0.670818164
barren	810	0	0
moderate to sparse vegetation	716739	174	-0.18890274
	2148389	630	

5.3 Weight of Evidence (WoE) Method

WoE is a Bayesian statistical model that evaluates the presence and absence of landslides with respect to conditioning factor classes. It computes two weights:

- $W^+ = \ln[(Si / Ni) / (S / N)]$
- $W^- = \ln[(1 - Si / Ni) / (1 - S / N)]$

The contrast value ($C_i = W^+ - W^-$) reflects the net effect of each class in causing landslides. The final susceptibility score is:

LSI = $\sum \text{Contrast}_i$

Contrast values were computed for each factor class and integrated using raster algebra. The WoE model accounts for both spatial presence and absence, making it suitable for comprehensive risk modelling.

Slope	**C**	**L**	**W^+**	**W^-**	**C**
<15	756385	42	-1.66	0.37	-2.03
15-25	690674	196	-0.03	0.02	-0.05
25-35	539808	274	0.55	-0.28	0.83
35-45	146356	107	0.91	-0.12	1.03
>45	15166	11	0.91	-0.01	0.92
ASPECT	**C**	**L**	**W PLUS**	**W MINUS**	**C**
Flat (-1)	0	0	0	0	0
North (0 - 22.5)	123021	27	-0.29	0.02	-0.31
Northeast (22.5 - 67.5)	269621	76	-0.04	0.01	-0.05
East (67.5 - 112.5)	250070	80	0.09	-0.01	0.10
Southeast (112.5 - 157.5)	218151	55	-0.15	0.02	-0.17
South (157.5 - 202.5)	264168	80	0.03	0.00	0.04
Southwest (202.5 - 247.5)	333155	130	0.29	-0.06	0.35
West (247.5 - 292.5)	321332	103	0.09	-0.02	0.11
Northwest (292.5 - 337.5)	260133	47	-0.48	0.05	-0.54
Northwest (292.5 - 337.5)	108738	32	0.00	0.00	0.00
Curvature	**C**	**L**	**W PLUS**	**W MINUS**	**C**
Convex	356185	132	0.23	-0.05	0.29
Flat	764299	176	-0.24	0.11	-0.35
Concave	1027905	322	0.07	-0.06	0.13
GEOMORPHOLOGY	**C**	**L**	**W PLUS**	**W MINUS**	**C**
Waterbody – River	31544	3	-1.13	0.01	-1.14
Highly Dissected Hills and Valleys	1532348	537	0.18	-0.66	0.84
Moderately Dissected Hills and Valleys	223359	60	-0.09	0.01	-0.10
Alluvial Plain	347204	30	-1.22	0.13	-1.35
Flood Plain	10914	0	0.00	0.01	-0.01
Anthropogenic terrain	564	0	0.00	0.00	0.00
Quarry and Mine Dump	2456	0	0.00	0.00	0.00
TWI	**C**	**L**	**W PLUS**	**W MINUS**	**C**
2.70-5.0	762752	356	0.46	-0.39	0.86
5.0-8.0	1080934	244	-0.26	0.21	-0.47
8.0-12.0	241558	26	-1.00	0.08	-1.08
12.0-16.0	52504	2	-2.04	0.02	-2.06
16-23.72	10641	2	-0.44	0.00	-0.45
SPI	C	L	W PLUS	W MINUS	C
-1.52288	76066	0	0.00	0.04	-0.04
0-2.0	1615313	498	0.05	-0.17	0.22
2.0-4.0	433668	129	0.01	0.00	0.02
4.0-6.0	22929	2	-1.21	0.01	-1.22
6.0-7.01	413	1	2.11	0.00	2.11
Lineament distance	**C**	**L**	**W PLUS**	**W MINUS**	**C**
0-250	309340	106	0.16	-0.03	0.18
250-500	273762	89	0.10	-0.02	0.12
500-750	246615	50	-0.37	0.04	-0.41
750-100	219621	42	-0.43	0.04	-0.47
1000 ABOVE	1099051	343	0.06	-0.07	0.13
ROAD	**C**	**L**	**W PLUS**	**W MINUS**	**C**
0-50	398733	522	1.29	-1.69	2.99
50-100	321487	62	-0.62	-0.09	-0.54
100-150	265797	12	-2.08	-0.04	-2.03

150-200	182428	12	-1.70	-0.10	-1.60
200-250	192690	9	-2.04	-0.09	-1.96
250 above	787254	13	-3.08	0.39	-3.47
SOIL TYPE	**C**	**L**	**W PLUS**	**W MINUS**	**C**
Orthic Luvisols (Lo)	466582	16	-2.15	0.22	-2.37
Eutric Regosols (Re)	218832	62	-0.03	0.00	-0.04
Eutric Cambisols (Be)	1462454	552	0.25	-0.95	1.20
Dystric Cambisols (Bd)	521	0	0.00	0.00	0.00
NDVI	**C**	**L**	**W PLUS**	**W MINUS**	**C**
-0.019 – 0.041	5978	0	0.00	0.00	0.00
0.042 – 0.120	374140	50	-0.79	0.11	-0.89
0.121 – 0.183	605775	237	0.29	-0.14	0.43
0.184 – 0.242	724739	225	0.06	-0.03	0.09
0.243 – 0.438	437757	118	-0.08	0.02	-0.10
NDBI	**C**	**L**	**W PLUS**	**W MINUS**	**C**
-0.292 to -0.163	421756	152	0.21	-0.06	0.26
-0.162 to -0.122	628600	213	0.14	-0.07	0.21
-0.121 to -0.081	535282	140	-0.11	0.04	-0.15
-0.080 to -0.038	400747	97	-0.19	0.04	-0.23
-0.037 to 0.286	162004	28	-0.53	0.03	-0.56
NDWI	**C**	**L**	**W PLUS**	**W MINUS**	**C**
-0.409 to -0.238	214690	61	-0.03	0.00	-0.04
-0.237 to -0.186	428933	136	0.08	-0.02	0.10
-0.185 to -0.141	572580	163	-0.03	0.01	-0.04
-0.140 to -0.092	521201	202	0.28	-0.11	0.39
-0.091 to -0.066	410985	68	-0.57	0.10	-0.67
DRAINAGE DISTANCE	**C**	**L**	**W PLUS**	**W MINUS**	**C**
0-250	724460	208	-0.02	0.01	-0.03
250-500	572537	151	-0.11	0.04	-0.14
500-750	434254	130	0.02	-0.01	0.03
750-1000	279334	102	0.22	-0.04	0.26
1000 ABOVE	137804	39	-0.04	0.00	-0.04
Rainfall Range (mm)	**C**	**L**	**W PLUS**	**W MINUS**	**C**
5,487.515 – 5,804.319	285362	17	-1.59	0.12	-1.71
5,804.32 – 6,054.698	436107	216	0.52	-0.19	0.72
6,054.699 – 6,269.308	583849	210	0.20	-0.09	0.29
6,269.309 – 6,483.918	657361	146	-0.28	0.10	-0.38
6,483.919 – 6,790.504	185710	41	-0.28	0.02	-0.31
LITHOLOGY	**C**	**L**	**W PLUS**	**W MINUS**	**C**
KROL	61321	18	0.00	0.00	0.00
BALIANA	108360	41	0.25	-0.02	0.27
SIMLA	301602	79	-0.11	0.02	-0.13
SHALI	123922	9	-1.40	0.05	-1.44
SIRMUR = DHARAMSHALA	498951	235	0.47	-0.20	0.68
JAUNSAR	74753	5	-1.48	0.03	-1.51
JUTOGH	4495	2	0.42	0.00	0.42
DAGSHAI AND KASAULI (UNDIFF)	121834	101	1.04	-0.12	1.16
UNDIFFERENTIATED QUATERNARY	14030	1	-1.41	0.00	-1.42
NEWER ALLUVIUM	50792	6	-0.91	0.01	-0.92
SIWALIK	540760	132	-0.18	0.05	-0.24
OLDER ALLUVIUM	247569	1	-4.29	0.12	-4.41

ELEVATION	C	L	W PLUS	W MINUS	C
226-625	504604	31	-1.56	0.22	-1.78
625-1024	636384	204	0.09	-0.04	0.13
1024-1423	703752	267	0.26	-0.15	0.41
1423-1822	270978	125	0.45	-0.09	0.54
1822-2221	32671	3	-1.16	0.01	-1.17
Land Cover Class	**C**	**L**	**W PLUS**	**W MINUS**	**C**
Water Body	27939	4	-0.72	0.01	-0.72
Forest	894437	242	-0.08	0.05	-0.13
Agriculture	142314	0	0.00	0.07	-0.07
Built-up / Settlement	366150	210	0.67	-0.22	0.89
barren	810	0	0.00	0.00	0.00
moderate to sparse vegetation	716739	174	-0.19	0.08	-0.27

4. Results and Discussion

Landslide susceptibility maps for Solan District were prepared using three different statistical models: Frequency Ratio (FR), Information Value (IV), and Weight of Evidence (WoE). The results indicate a clear variation in how landslides are distributed across the region. The centre and southeastern sections, which are mostly found in high to extremely high hazard zones, are the most vulnerable. The accuracy of all models was evaluated using the Area Under the Curve (AUC) and Success Rate Curve (SRC) methods. The results highlighted the differences in predicting abilities of each model. The Frequency Ratio (FR) model with an AUC of 91.14% ,followed closely by the Information Value (IV) model with an AUC of 88.32%.and the WoE model with an AUC of 82.25%, all yielded trustworthy results.

Figure 7 WoE, IV, and FR Method LSZ Maps and Success Curve.
(Source : Author)

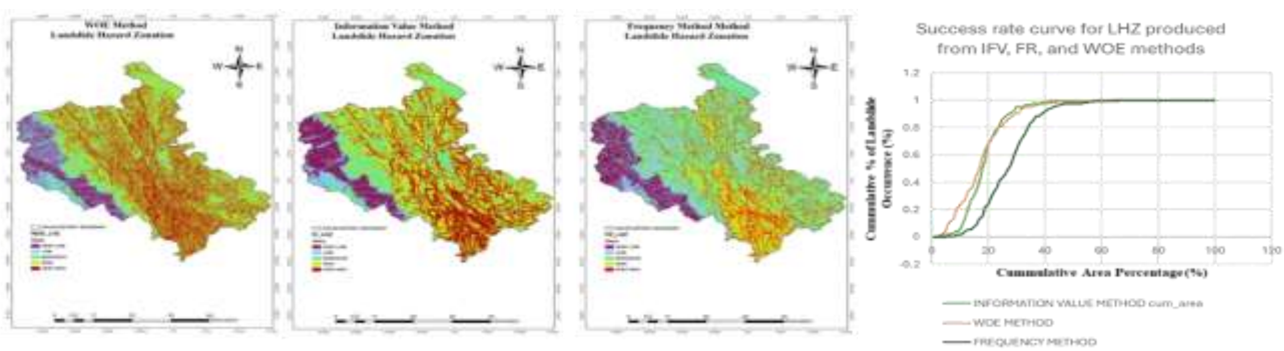

Figure 8 Analysis of thematic layer data and findings from the FR, Woe, and IV techniques.
(Source: Author)

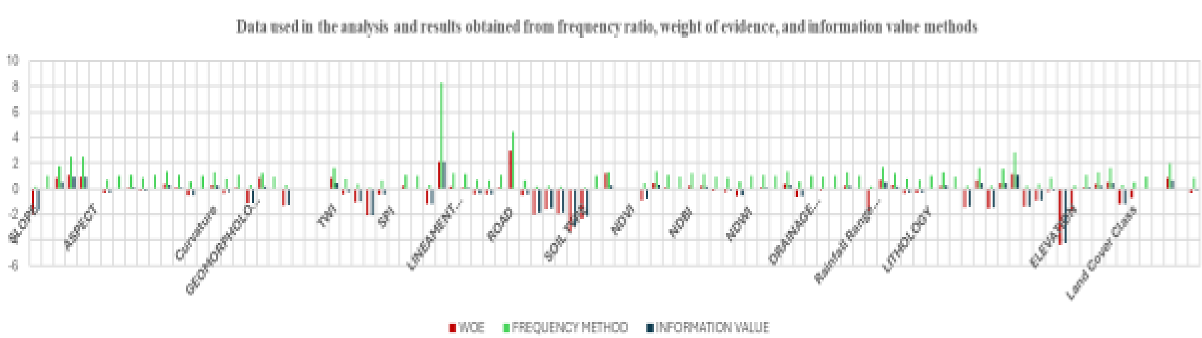

4.1 Frequency Ratio Model Interpretation

The Frequency Ratio (FR) method is a statistical approach for assessing landslide frequency by comparing the spatial relationship between landslide occurrences and various causative factors. The FR values indicate that slope is a dominant factor, highlighting the slope instability in steeper terrains. Slope classification 35–45° (FR=2.49) and classification >45° (FR=2.45) recording the highest FR values. The Aspect value (FR = 1.33) indicated that the southwest-facing slopes were the most susceptible. This is potentially due to increased solar exposure and weathering compared to the western- and southern-facing slopes. Both concave (FR= 0.63) and convex (FR=1.26) slopes influence landslides. Concave slopes accumulate water while convex slopes promote erosion and runoff. Highly dissected hills and valleys in geomorphology recorded the highest FR (1.19), which aligned with zones of active erosion and geomorphic instability. Drainage proximity within the 750–1000 m classification showed elevated susceptibility (FR = 1.24) due to hydrological influences, such as subsurface water flow and toe cutting. The area within 0–50 m from roads had a significantly high FR of 4.46. Hence, road proximity was also a key anthropogenic factor underscoring the destabilizing impact of excavation and slope modification. Vegetation indices with moderate NDVI values (0.121–0.183) showed the highest FR (1.33) indicating that partially vegetated areas are more prone to landslides. NDWI values ranging from -0.140 to -0.092 had a peak FR of 1.32, suggesting that moisture-rich zones are more unstable. Built-up areas in NDBI were identified as high risk zone due to high FR values (FR > 1.22). This is due to anthropogenic interventions leading to impervious surfaces and altered drainage. In Soil study, Eutric Cambisols recorded the highest FR (1.29) with moderate soil permeability and a higher saturation potential. Lithological data showed that Dagshai and Kasauli formations (undifferentiated) had the maximum FR (2.82) due to their fractured, weathered and structurally weak characteristics. Elevation zones between 1423 and 1822 m exhibited the highest FR (1.57), indicating that mid-altitude areas with steep slopes and high rainfall are more vulnerable to landslides. The Land use/land cover (LULC) study highlighted that built-up zones had an FR of 1.95 due to intense anthropogenic pressure on such terrains. Whereas the forest and sparse-vegetation zones showed moderate susceptibility. Rainfall intensity in the range of 5804–6054 mm/year, corresponded with the highest FR (1.68). The rainfall study reinforced the critical role of monsoonal downpours in triggering landslides. Overall, the Frequency Ratio model successfully delineates zones of varying landslide susceptibility. The model provided valuable insights into the relationships between environmental variables and historical landslide patterns in the Solan district.

Figure 9 Landslide Hazard Zonation FR Method

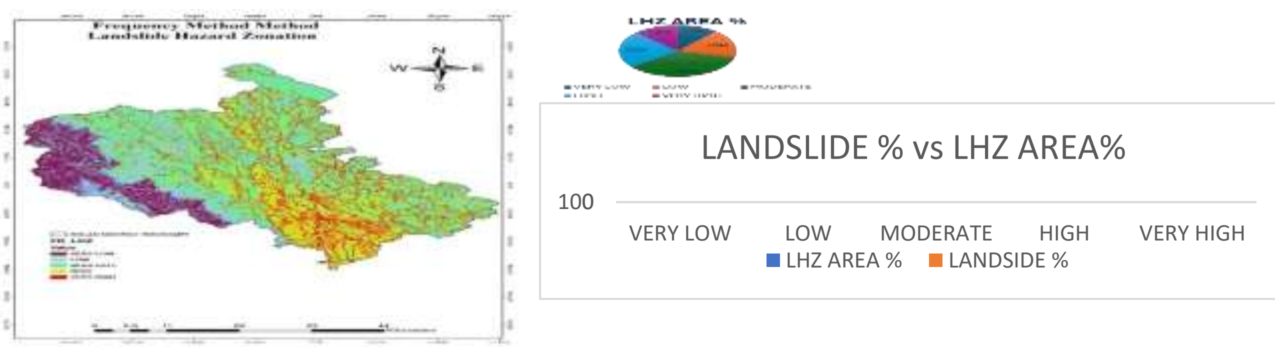

The study region was divided into five landslide susceptible hazard zones as very low, low, moderate, high, and very high. With 35% of the overall area is under a moderate susceptibility zone. This zone indicated that more than one-third of the area is at intermediate risk of landslides due to a mix of human and natural factors. The high susceptibility zone comprises 23% of areas where steep slopes, altered land use and lithological instability significantly elevate landslide potential. The low susceptibility zone accounted for 18% of the area. This represents more stable terrain, likely due to favourable slope angles, vegetation cover, or limited disturbance. The very high susceptibility zone accounted for 13% of the area and likely corresponded to the most unstable regions. These areas are predominantly characterized by steep terrain, weak lithology and intensive human activities such as road construction or deforestation. The very low-susceptibility zone (11% of the total area) indicated relatively stable areas with gentle slopes and minimal external disturbance. An Area Under the Curve (AUC) study was conducted to assess the model's prediction capacity. The results depicted a score of 0.9114. The output indicated high accuracy in validating the reliability of the Frequency Ratio approach for locating areas in the Solan district that are vulnerable to landslides.

4.2 Information Value (IV)

The interpretation of the Information Value model for landslide susceptibility mapping in Solan District showed a thorough statistical correlation between several causal elements and past landslide occurrences. Slope steepness has a significant impact on landslide probability classes between 35–45° (IV= 0.91) and >45° (IV=0.90). Slope reflected the highest IV values among topographic characteristics. The highest IV value in aspect was found on southwest-facing slopes (0.29) also highlighted the vulnerability of slopes to weathering and solar exposure. Curvature analysis indicated that concave zones were the most influential (IV = 0.07) and consistent with their tendency to accumulate runoff. Highly dissected hills and valleys in geomorphology assessment exhibited the highest positive IV (0.18) which indicated their vulnerability to active erosional processes. TWI values between 2.7–5.0 (IV = 0.46) indicated increased landslide activity in moderately wet areas. SPI values between 6–7 with high IV (2.11) indicated an extreme landslide susceptibility in regions with high surface runoff accumulation. In terms of proximity to lineaments and roads, areas within 250 m of roads had a strong influence (IV values above 4.46) underscoring anthropogenic slope disturbance. In Soil study, Eutric Cambisols registered the highest IV (0.25) while Orthic Luvisols recorded strong negative influence (–2.14). The NDVI class 0.121–0.183 which depicts the sparse vegetation showed the highest vegetation-related IV (0.29), whereas denser vegetation showed a negative correlation. Similarly, NDWI values between –0.140 to –0.092 showed high IV (0.2) which highlights the role of soil moisture in slope destabilization. The undifferentiated formations of Dagshai and Kasauli in lithology study exhibited the highest IV (1.03), reflecting their weathered and weak structures. Elevations between 1423–1822 m showed the highest susceptibility (IV = 0.45) aligned with steeper mid-hill terrain. IV values in Built-up areas (0.067) in the land cover study confirmed that intense human activity is a primary destabilizing agent. Rainfall amounts between 5804–6054 mm showed the highest IV (0.52), validating precipitation as a major landslide trigger in the monsoon-prone Solan region. Altogether, the IV model effectively distinguishes between high- and low-contributing factors while providing a granular understanding of landslide dynamics essential for disaster mitigation and slope management.

Figure 10 Landslide Hazard Zonation IV Method

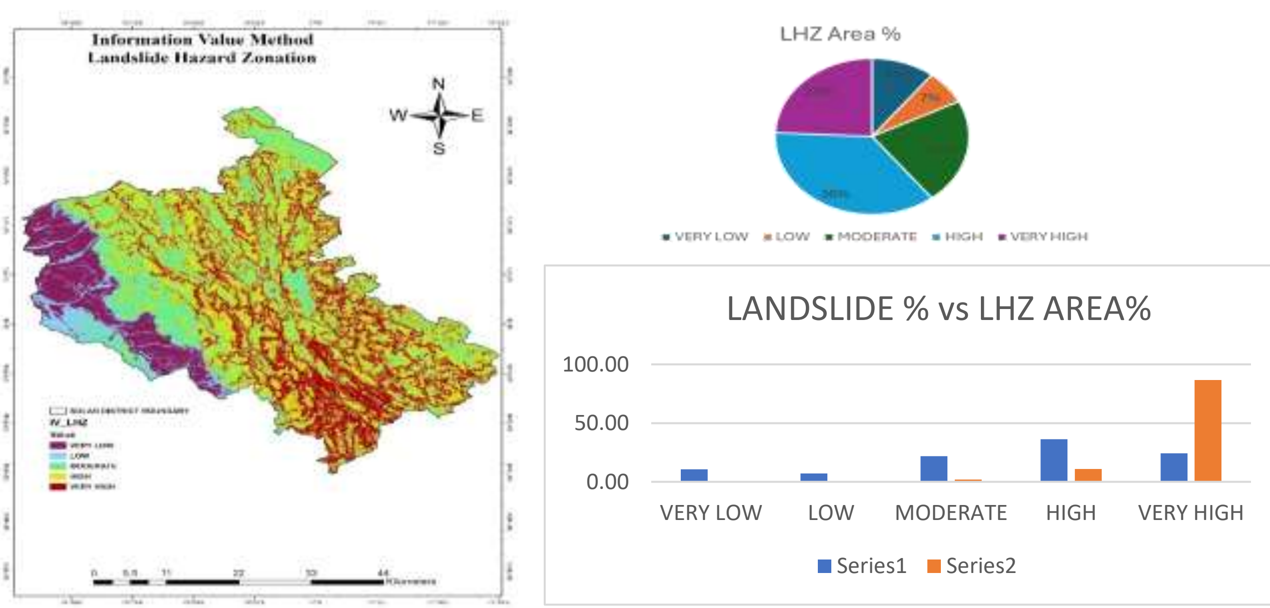

The study area was divided into five landslide susceptibility zones using the Information Value model. The high susceptibility zone covered 38.1% of the region and this substantial proportion reflects the widespread nature of terrain that is prone to slope failure. The primary causes include steep gradients, active geomorphic processes, and growing human disturbances. The very high susceptibility zone accounted for 25.4% of the Solan district, as these areas contain the most critical slopes where landslides occur frequently due to deeply weathered and structurally weak bedrock. The moderate class covered 23.1% of the study area and serves as a transition zone where human activities interact with the surrounding environmental conditions. The low and very low susceptibility zones accounted for only 7.4% and 1.1% of the district, respectively. These zones are typically found on gentler terrain or within stable geological formations where disturbance remains minimal. The model was tested against actual landslide events, and 140 landslides were identified within the higher-risk zones. This concentration confirms that the model aligns well with real-world conditions. To further evaluate predictive performance, the study used an Area Under the Curve analysis, with an AUC value of 0.883. This strong score demonstrates that the Information Value model is both robust and reliable for identifying landslide-prone areas. The method also offers practical value for regional planning and disaster risk reduction efforts.

4.3 Weight of Evidence (WoE) Model Interpretation

The Weight of Evidence model highlighted the spatial correlation between landslide occurrences and causative factors across the Solan district. Slope (above 25°, 35–45° and >45°) exhibited strong positive weights (W+ > 0.9). This confirms that slope plays a critical role in landslide hazards due to gravitational instability on steeper terrains. The southwest and west-facing slopes, with weights W+ = 0.28 and 0.089 for slope aspect, indicated moderate susceptibility. This is influenced by sun exposure and weathering patterns. Convex slopes in curvature map showed a distinctly higher positive weight (W^+ = 0.23). This pattern indicates that outward-curving landforms tend to gather more surface runoff causing slope failure or small-scale mass movement. The severely dissected hill and valley systems in geomorphology had a significant positive weight (W^+ = 0.178) were the most landslide-prone locations. Zones formed by human activity or alluvial processes in LULC study depicted no impact and occasionally even showed negative weights. Zones with moderate wetness (2.7–5.0) demonstrated significantly higher susceptibility (W+ = 0.46) in TWI analysis. This indicated that the ideal soil moisture levels are also favourable to failure. Whereas, high SPI class 6.0–7.01 yielded a substantial W+ of 2.11, depicting the role of concentrated runoff zones. Proximity to roads highlighted a dominant anthropogenic trigger. The areas within 50 meters of roads recording the highest W+ (1.29) and contrast C = 2.98. This confirmed that the destabilizing impact of road cuts and drainage alterations leading to slope failures. Orthic Luvisols (Lo) soil had a strong negative influence and Eutric Cambisols (Be) soil registered the strongest connection (W+ = 0.25, C = 1.20). In terms of vegetation indices, higher landslide occurrence (W+ = 0.29) was linked to moderate NDVI values (0.121–0.183). This indicates scant or degraded plant cover. The largest discrepancy between land cover classes was seen in built-up and settlement regions (W+ = 0.67, C = 0.89). The values suggestes a substantial human inventions caused landslide hazards. Higher weights (W+ = 0.22) in drainage proximity (750–1000 m) indicated that transitional runoff zones are more sensitive to slope failures. Additionally, elevation ranges between 1423 and 1822 m had a positive correlation (W+ = 0.45). The WoE model successfully represented the multifactorial nature of landslide susceptibility as it confirms the spatial importance of both natural and man-made factors. These interpretations support the predictive reliability of the model and offer crucial information for development controls and slope stabilisation planning in susceptible areas.

Figure 11 Landslide Hazard Zonation WOE Method

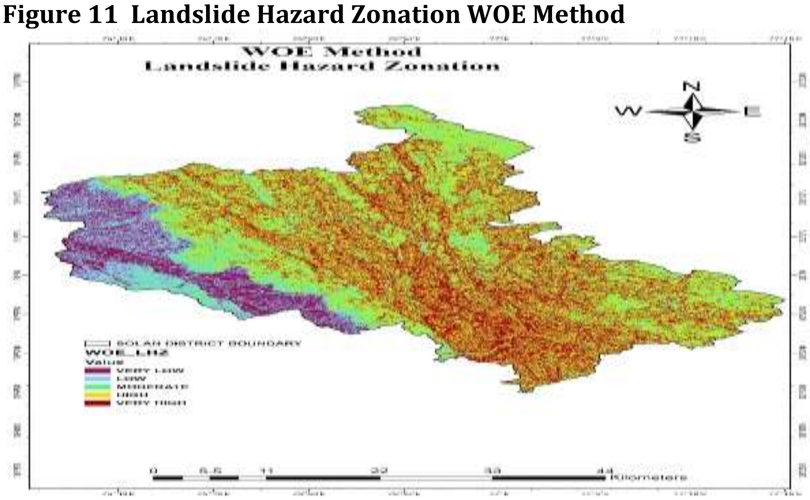

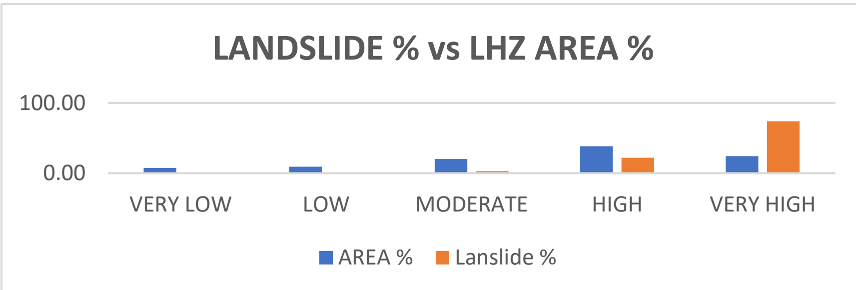

The landslide susceptibility zonation (LSZ) map generated using the Weight of Evidence (WoE) method was categorized into five susceptibility zones: very low, low, moderate, high and very high. The high-susceptibility zone accounted for the largest portion of the landscape (40.3%). This reflected that the terrain was characterized by steep slopes, anthropogenic alterations and geologically weak formations. About 25.5% of the region was in the very high susceptibility zone with the highest concentration of landslide activity. About 21.5% of the area was in the intermediate zone. This denoted transitional terrain with moderate vulnerability impacted by a combination of environmental and geological variables. About 12.7% of the region was in the low and very low zones combined, indicating few or no landslides. When the hazard pattern was analyzed, the zones marked as "very high" susceptibility contained most of the mapped landslide pixels. This highlighted a strong link between the WoE output and actual slide locations. To assess the model's reliability ,the AUC-ROC curves were generated. The Area Under the Curve value was 0.89. High AUC value shows that the model distinguishes well between stable and unstable slopes. Hence, it reliably locates landslide-prone areas and provides a sound basis for regional hazard planning and slope management efforts.

5. Conclusion

This research analydsed landslide susceptibility in the Solan district using three statistical approaches: Information Value, Weight of Evidence and Frequency Ratio method. An elaborated landslide inventory was developed through the interpretation of satellite imagery, field validation and high-resolution datasets. Seventeen causative factors such as slope, aspect, curvature, geomorphology, lithology, land use/land cover, soil type, hydrological indices (SPI, TWI, NDVI, NDWI), rainfall patterns, elevation, and proximity to roads and drainage networks were systematically integrated into the modelling framework. The final Landslide Susceptibility Zones (LSZ) maps were classified into five groups: very low, low, moderate, high, and very high. The analyses highlighted that the FR model demonstrated the highest landslide predictive performance with an AUC value of 91.14% among the IV model (AUC 88.32%) and the WoE model (AUC 82.25%). The high AUC values validate the dependability of the susceptibility zonation outputs. While the very low and low susceptibility zones correlated with more stable areas and the very high susceptibility zone accurately reflected the densest concentration of reported landslides. While many areas fall under medium to high landslide risk, the steep slopes are the most landslide- region.

The Weight of Evidence (WoE) analysis identified landslide-susceptible zones. These locations consistently record the highest likelihood of landslide activity as compared with the rest in Information Value (IV) models. The consistency in the results of both models gave greater confidence in the reliability of the analysis. Among all the approaches, the FR model depicted the spatial variation of landslides more effectively. This methodology and its results can help experts working in hilly-area development planning and disaster management make more informed decisions on the ground. Utilizing these approaches in land-use planning practices by overlapping risk areas will help to protect both people and the landscape.

Acknowledgment

I would like to thank Dr. Kanwarpreet Singh, Associate Professor at Chandigarh University (University Centre for Research and Development (UCRD) Mohali, Punjab), for his constant guidance throughout this study. His insightful comments and encouragement have played a vital role in the successful completion of this research.

Conflict of Interest Statement

The authors declare no conflict of interest in this research paper.

References

1. (NIDM), N. I. (2020). National Landslide Risk Management Strategy. Ministry of Home Affairs, Government of India.
2. Abdullah H. Alsabhana, K. S. (2022). Landslide susceptibility assessment in the Himalayan range based on the Kasauli – Parwanoo road corridor using weight of evidence, information value, and frequency ratio. Journal of Earth System Science.
3. Adil Ahmad Magray, K. S. (2023). Comparative analysis of certainty factor and analytic hierarchy process for landslide susceptibility zonation in parts of Solan, Himachal Pradesh, India. Quaestiones Geographicae, 5-18.
4. Adil Ahmad Magray, K. S. (2023). Comparative Analysis of Certainty Factor and Analytic Hierarchy Process for Landslide Susceptibility Zonation in Parts of Solan, Himachal Pradesh, India. QUAESTIONES GEOGRAPHICAE.
5. Anbalagan, R. K. (2015). Landslide susceptibility zonation in part of Tehri reservoir region using frequency ratio, fuzzy logic and GIS. Journal of Earth System Science, 431–448.
6. Bharat Prasad Bhandari, S. D.-Y. (2024). Assessing the Prediction Accuracy of Frequency Ratio, Weight of Evidence, Shannon Entropy, and Information Value Methods for Landslide Susceptibility in the Siwalik Hills of Nepal. Sustainability.
7. GSI. (2023). Risk Mapping of Hilly Areas under the National Landslide Susceptibility Mapping (NLSM) Programme. Government of India, Ministry of Environment, Forest and Climate Change.
8. HPSDMA. (2023 & 2024). Revised MEMORANDUM OF DAMAGES DUE TO FLASH FLOODS, FLOODS CLOUDBURSTS AND LANDSLIDES DURING MONSOON SEASON – .
9. Kumari Sweta, A. G. (2022). Performance assessment for three statistical models of landslide susceptibility zonation mapping: A case study for Dharamshala Region, Himachal Pradesh, India. Journal of Earth System Science.
10. Lalit Pathak, B. B. (2025). Landslides in the Himalayas: The Role of Conditioning Factors and Their Resolution in Susceptibility Mapping. Geosciences .
11. Mahesh Sharma, S. D. (2024). Preliminary assessment of the Shiv Bawdi landslide in Shimla, Himachal Pradesh, India. Recent Landslides, 1591–1601.
12. Petley, M. J. (2018). Global fatal landslide occurrence from 2004 to 2016. Natural Hazards and Earth System Sciences, 2161–2181.
13. Pham Viet Hoa, N. Q. (2023). GIS-based modeling of landslide susceptibility zonation by integrating the frequency ratio and objective–subjective weighting approach: a case study in a tropical monsoon climate region. Front. Environ. Sci.
14. Saibal Ghosh, C. V. (2012). Integrating spatial, temporal, and magnitude probabilities for medium-scale landslide risk analysis in Darjeeling Himalayas, India. Landslides, 371-384.
15. Tesfaldet Sisay, G. T. (2024). Landslide susceptibility mapping using combined geospatial, FR and AHP models: a case study from Ethiopia's highlands. Discover Sustainability.
16. Thakur, A. (2025). Sustainable urban policy development in hill cities: A case study of Shimla's LULC changes and urban regeneration efforts. Urban Governance.
17. Valdiya, K. (1980). Geology of the Kumaun Lesser Himalayas. . Dehradun: Wadia Institute of Himalayan Geology.
18. Vipin Chauhan, L. G. (2024). Landslide susceptibility assessment for Uttarakhand, a Himalayan state of India, using multi-criteria decision making, bivariate, and machine learning models. Geoenvironmental Disasters, 1-17.
19. Yuqian Yang, X. W. (2024). Optimal statistical method selection for landslide susceptibility assessment and its scale effect. Sec. Geohazards and Georisks.
20. Zare, V. V. (2014). Landslide susceptibility mapping by comparing the weight of evidence, fuzzy logic, and frequency ratio methods. Geomatics, Natural Hazards and Risk.